Journal of Hydrology xxx (xxxx) xxxx

Contents lists available at ScienceDirect

Journal of Hydrology

journal homepage: www.elsevier.com/locate/jhydrol

Research papers

Biogeochemical and physical controls on the evolution of dissolved inorganic carbon (DIC) and $\delta^{13}C_{DIC}$ in karst spring-waters exposed to atmospheric $CO_{2(g)}$: Insights from laboratory experiments

Yongjun Jiang[a,*], Jiaqi Lei[a], Liuchan Hu[a], Qiong Xiao[b], Jinliang Wang[b], Cheng Zhang[b], Hendratta Ali[c]

[a] Chongqing Key Laboratory of Karst Environment & School of Geographical Sciences of Southwest University, Chongqing 400715, China
[b] Key Laboratory of Karst Dynamics, MLR & Guangxi, Institute of Karst Geology, Chinese Academy of Geological Sciences, Guilin 541004, China
[c] Department of Geosciences, Fort Hays State University, Hays, KS 67601, USA

ARTICLE INFO

This manuscript was handled by Huaming Guo, Editor-in-Chief, with the assistance of Philippe Negrel, Associate Editor

Keywords:
Dissolved inorganic carbon
Stable carbon isotope
Biological process
Chemical process
Physical process
Karst spring-waters-atmosphere interaction

ABSTRACT

Karst waters (spring-fed streams, lakes and reservoirs) characterized by relatively high concentrations of dissolved inorganic carbon (DIC) and p_{CO_2} significantly impact regional and global carbon cycles by releasing carbon dioxide to the atmosphere. Investigating the transfer of DIC from karst waters to the atmosphere is important to further our understanding of carbon cycling in karst environments. There is still considerable uncertainty about the controls of DIC transfer in karst waters because of challenges associated with investigations that aim to mimic the continuum of changes in DIC concentrations to equilibrium with atmospheric CO_2 in natural settings. Laboratory simulations can create controlled conditions that allow targeted investigations. In this study, four tanks were taken to investigate the variations of pCO_2, DIC and $\delta^{13}C_{DIC}$ when karst spring-waters were exposed to the atmosphere from 40 to 360 h as: (1) agitated water containing *Hydrilla verticillata*; (2) static water containing *Hydrilla verticillata*; (3) agitated water without *Hydrilla verticillata*; and (4) static water without *Hydrilla verticillata*. The rates of photosynthesis/respiration of submerged plants, CO_2 outgassing and carbonate precipitation/dissolution were quantified by a time-stepping chemical/isotopic mass balance model. This experiment was designed to create ideal conditions to estimate the temporal evolution of DIC and $\delta^{13}C_{DIC}$, and investigate mechanisms that control their evolution when karst spring-waters interact with atmospheric CO_2. Results show: (1) generally a steep decrease in DIC concentrations and $\delta^{13}C_{DIC}$ enrichment; (2) DIC loss and $\delta^{13}C_{DIC}$ enrichment are faster in the agitated waters with submerged plants; (3) DIC evolution is mainly controlled by the metabolism of aquatic plants; (4) carbonate precipitation/dissolution and CO2 outgassing has a lower effect on the DIC evolution in waters with submerged plants; (5) $\delta^{13}C_{DIC}$ evolution is mainly controlled by the metabolism of submerged plants; (6) CO_2 evasion, photosynthesis and $\delta^{13}C_{DIC}$ enrichment are accelerated by the agitation of waters. Our analyses show that more than 40% of the total DIC resulting from carbonate weathering was used for photosynthesis by submerged aquatic plants thereby transforming the DIC into organic carbon (OC), suggesting that intense aquatic photosynthetic activities in continental surface water systems could play an important role as natural carbon sinks.

1. Introduction

Continental waters, such as rivers and streams, are important links in the global carbon cycle long considered to be passive “pipes” and conduits in carbon budgets and weathered products of carbonate rocks (Schlesinger and Melack, 1981). However, recent findings suggest an alternative view that the carbon discharged to the oceans is only a fraction of the total carbon entering rivers from terrestrial ecosystems. Most of the influx of carbon into rivers from soil respiration and physico-chemical weathering is (1) returned to the atmosphere through degassing, as $CO_{2(g)}$ before the rivers discharge into the ocean, (e.g. Richey et al., 2002; Cole et al., 2007; Battin et al., 2009; Aufdenkampe et al., 2011; Striegl et al., 2012; Raymond et al., 2013), due to the high CO_2 partial pressure (p_{CO_2}) in the rivers compared to atmospheric CO_2; and (2) sedimentary organic carbon (OC) buried in river deposits (e.g., Cole et al., 2007; Battin et al., 2009; Aufdenkampe et al., 2011), that

* Corresponding author.
E-mail address: jiangjyj@swu.edu.cn (Y. Jiang).

https://doi.org/10.1016/j.jhydrol.2019.124294
Received 1 April 2019; Received in revised form 21 October 2019; Accepted 28 October 2019
Available online 01 November 2019

accumulates over thousands of years and may eventually lithify, to constitute a relatively long-term natural carbon sink.

Current estimates suggest that 2.7 Pg C $year^{-1}$ of terrestrial C fluxes (organic and inorganic carbon) are exported to continental waters, of which 1.2 Pg C $year^{-1}$ are released to the atmosphere, 0.6 Pg C $year^{-1}$ are trapped in sediment, and only 0.9 Pg C $year^{-1}$ are delivered to the world's oceans (Aufdenkampe et al., 2011). However, there remain large uncertainties on the magnitude of C fluxes in global continental waters (Cole et al., 2007; Battin et al., 2009; Aufdenkampe et al., 2011; Liu, 2011).

Carbonate outcrops represent approximately 20% of the earth's ice-free surface (Ford & Williams 2007) and their rapid dissolution by carbonic acid increases the amount of dissolved inorganic carbon (DIC) species (HCO_3^-, CO_3^{2-}, H_2CO_3 and $CO_{2(aq)}$,) and calcium ions in karst ground- and surface waters. High concentrations of DIC, leading to a change in the pCO_2 in these karst waters (e.g. in aquifers, rivers, streams, reservoirs, and lakes), is a potential source for atmospheric CO_2, which could significantly impact the regional and ultimately the global carbon cycle (Liu, 2011; Martin, 2017). Thus, to address the uncertainties of C fluxes in global continental waters, it is necessary to investigate and assess the role of karst (carbonate) impacted surface water bodies like streams on DIC evolution. Ultimately, the transfer of DIC from sediments and waters to the atmosphere depends on the processes and concentrations that are locally at play.

Three principal processes that control DIC and $\delta^{13}C_{DIC}$ evolution in surface waters from karst spring-waters are: (1) physical water - air exchange, i.e. $CO_{2(g)}$ transfer to the atmosphere; (2) geochemical reactions involving carbonate precipitation and/or dissolution; and (3) biogeochemical processes involving respiration and photosynthesis. The extent of the effect of each process depends on hydrologic conditions (e.g. recharge/discharge, flow velocity, aquatic plant type and productivity, residence time, and ion saturation), underlying geology, climate and atmospheric conditions etc.

$CO_{2(g)}$ exchange is a physical flux driven by DIC concentrations, speciation reactions and relative the pCO_2 between water and the atmosphere. Surface waters with high DIC concentrations and higher pCO_2 will lose $CO_{2(g)}$ to the atmosphere as the waters evolve towards chemical equilibrium with atmospheric $CO_{2(g)}$. As a result of CO_2 evasion, increase the solubility of calcite, leads to saturation and $CaCO_3$ precipitation from the solution (e.g. Jacobson and Usdowski, 1975; Dreybrodt et al., 1992).

Metabolic reactions by submerged plants can force diel cycles of DIC in waters, especially in karst waters with high pCO_2 (Parker et al., 2007, 2010; de Montety et al., 2011; Gray et al., 2011; Nimick et al., 2011; Tobias & Böhlke, 2011; Jiang et al., 2013; Peter et al., 2014; Liu et al., 2015; Chen et al., 2017; Pu et al., 2017). Calcite precipitation due to the joint effect of chemical and biological processes can be represented by Eq. (1) (Smith and Gattuso, 2011).

$$Ca^{2+} + 2HCO_3^- \leftrightarrow CaCO_3\downarrow + x\,(CH_2O + O_2) + (1-x)(CO_2\uparrow + H_2O) \quad (1)$$

Thus, in addition to being a source for atmospheric CO_2, high concentrations of DIC and pCO_2 in karst waters can also be the C source for photosynthesis of submerged plants, converting DIC into organic carbon. With time, some of the organic carbon could eventually be buried and converted into autochthonous organic matter as a long-term or permanent carbon sink (Cole et al., 2007; Einsele et al., 2001).

In these karst water systems, the $\delta^{13}C_{DIC}$ in the evolving DIC waters will change because of the isotopic fractionation accompanying carbon loss/gain (degassing to the atmosphere, calcite precipitation/dissolution and carbon assimilation/disassimilation during metabolism) from the system (e.g. Clark and Fritz,1997; Parker et al., 2007; Tobias & Böhlke, 2011; Abongwa and Atekwana, 2013, 2015; Jiang et al., 2013; Khadka et al., 2014; Liu et al., 2015; van Geldern et al., 2015; Pu et al., 2017). The resulting $\delta^{13}C_{DIC}$ of the karst waters can thus be described by either kinetic or equilibrium isotope fractionation (Zhang et al., 1995). Although DIC evolution in surface waters tends towards chemical and isotopic equilibrium with the atmosphere, it is challenging, especially in karst waters, to map this kind of DIC evolution. These challenges result from complications due to the complexity of reaction pathways and large variations in field settings. Thus far, isotopic disequilibrium appears to be the rule especially for field-based investigations of karst waters to date. Laboratory experiments (e.g. Abongwa and Atekwana, 2013, 2015) can provide near ideal ways to assess how the DIC and $\delta^{13}C_{DIC}$ of karst waters evolve to chemical and isotopic equilibrium with the atmosphere.

In this study, the temporal evolutions of DIC and $\delta^{13}C_{DIC}$ were assessed in karst spring-waters treated to different hydro-biological conditions and exposed to attain equilibrium with the atmosphere in a laboratory setting. The objectives are to (1) document how the DIC and $\delta^{13}C_{DIC}$ in karst spring-waters exposed to atmospheric $CO_{2(g)}$ evolve under agitated and static conditions with/without aquatic plants, and (2) determine the effect of physical, chemical and biological processes on the evolution of DIC and $\delta^{13}C_{DIC}$ in karst spring-waters exposed to atmospheric $CO_{2(g)}$.

2. Experimental design and methods

2.1. Experimental design

Four tanks were prepared with different treatments to address the hydro-biological conditions for investigation as follows: two tanks with 465 g ± 2.5 g of contain a common submerged macrophyte in karst environments, *Hydrilla verticillata* (e.g. Sousa, 2011), collected from an experimental pool on the campus of the Southwest University, and two other tanks treated with ClO_2 were mixed with 1 L of a 2.5 mg/L ClO_2 solution to eliminate microbial activity. One tank from each set (treated with *Hydrilla verticillata* and ClO_2) was subjected to agitation by continuously circulating the water at a rate of 14 L/min using a submersible pump (to simulate turbulent flow conditions) and the other tanks were maintained under static conditions (to simulate laminar flow or steady conditions) (Table 1).

Unfiltered and untreated water was collected from Chongqing Qingmuguan karst spring (106°20′10″E, 29°47′00″N) around 8:00 a.m. on July 7th, 2015, in 80 L tightly sealed (headspace free) tanks and transported within 15 min to the laboratory. Under laboratory conditions, the water was transferred by pumping into four smaller (63 cm × 45 cm), acid pre-washed plastic tanks (WT1, WT2, WT3 and WT4), and immediately measured for physicochemical parameters. The initial measurements of the unfiltered/untreated water are reported in Table 2. After initial measurements, the water samples were then subjected to hydro-biological, and chemical treatments, as shown in Table 1.

All four tanks were exposed under the same atmospheric conditions for the duration of the experiment, by placing them on the roof of the building of the School of Geographical Sciences. The duration of the experiments depended on the time required by each tank to reach chemical and isotopic equilibrium with atmospheric $CO_{2(g)}$. As a consequence, the experiments lasted between 48 and 360 h depending on the time it took for the waters to reach chemical and isotopic equilibrium with atmospheric $CO_{2(g)}$. The experimental setup of the four tanks is shown in Fig. 1.

Table 1
The basic conditions and duration of experiment for each tank.

Tank ID	WT1	WT2	WT3	WT4
Hydrilla verticillata (465 g)	✓	✓	×	×
Agitation (14 L/min)	✓	×	✓	×
Reagent	×	×	ClO_2 solution	ClO_2 solution
Duration of experiment (h)	48	48	96	360

Table 2
Initial values of chemistry and $\delta^{13}C_{DIC}$ of karst spring-water for all 4 tanks.

T °C	pH	SpC μS/cm	DO mg/L	Ca^{2+} mg/L	Mg^{2+} mg/L	K^+ mg/L	Na^+ mg/L	HCO_3^- mg/L	SO_4^{2-} mg/L	NO_3^- mg/L	Cl^- mg/L	p_{CO_2} ppmv (water)	p_{CO_2} ppmv (air)	$\delta^{13}C_{DIC}$ (‰)
20.4	7.25	650	8.05	120	16.9	2.6	3.1	329.4	18.0	19.7	7.1	16,500	410	−10.9

2.2. Measurements, sampling and laboratory analyses

2.2.1. Measurements

Two WTW Technology MultiLine 340 multi-probes and two HACH multi-parameter data loggers were programmed to regularly measure pH, water temperature (T), dissolved oxygen (DO) and specific conductivity (SpC) at 15 min interval from the start to the end of the experiment. Prior to measurements, the instruments were calibrated according to manufacturer specification. The precision on pH, DO, T and SpC are 0.01, 0.01 mg/L, 0.01 °C and 1 μS/cm, respectively. Atmospheric CO_2 was measured at 15 min intervals using a GMP22 carbon dioxide probe (Vaisala, Finland), and the p_{CO_2} in the waters were also measured at 15 min intervals using four GMP22 carbon dioxide probes fitted with films that prevent water from entering the probes, but allow CO_2, with a resolution of 1 ppmv.

In situ, HCO_3^- (CO_3^{2-}) and Ca^{2+} concentrations were determined by test kits using a titration pipette (Aquamerck) with resolutions of 0.1 mmol/L and 1 mg/L, respectively, at 1 h intervals for the first 48 h. The measurements and samplings of tanks WT1 and WT2 ended after 48 h. Measurements of HCO_3^- (CO_3^{2-}) and Ca^{2+} ions were continued for tanks WT3 and WT4 until equilibrium was reached after 96 and 360 h, respectively. Sampling intervals were determined from variations in DIC concentrations. Sampling times are reported in Table S1.

2.2.2. Sampling and laboratory analyses

Water samples for measuring anion species were collected using syringes and immediately filtered through 0.45 μm filter membranes into pre-rinsed plastic containers. NO_3^- and SO_4^{2-} were determined by ultraviolet–visible spectrometry, and Cl^- was analyzed by titration with silver nitrate. The precision of all anion measurements is 0.01 mg/L. For major cation measurements (K^+, Na^+ and Mg^{2+}), water samples were collected in 100 mL plastic containers pre-acidified with HNO_3 to pH < 2.0. Cations were analyzed by an Inductively Coupled Plasma Optimal Emission Spectrometer (ICP-OES) with a resolution of 0.01 mg/L, at Chongqing Key Laboratory of Karst Environment (Southwest University).

Samples collected for $\delta^{13}C_{DIC}$ measurements were filtered through 0.45 μm membrane, to which 2 drops of a saturated solution of $HgCl_2$ were added. Using the modified method by Atekwana and Krishnamurthy (1998) for stable carbon isotope analysis of dissolved inorganic carbon, a 10 mL water sample was injected by syringe into glass bottles that were pre-filled with 1 mL 85% phosphoric acid and magnetic stir bars. The CO_2 in the samples was extracted and purified after cryogenic removal of H_2O using a liquid nitrogen–ethanol trap. Finally, the extracted CO_2 was transferred cryogenically into a tube for isotope measurement. The $\delta^{13}C_{DIC}$ were measured by Delta plus XL Gas stable isotope mass spectrometry. For the $\delta^{13}C_{CO2}$ of atmospheric gas, samples were collected from the air around the tanks in the mornings and afternoons using an evacuated glass vessel from July 7 to 13, and measured by Trace-Gas gas sample concentration system linked with an Isoprime-100 mass spectrometer. The *Hydrilla verticillata* samples were ultrasonically cleaned for 15 min in deionized water, and dried in an oven at 50 °C for 48 h. After drying, the plant samples were ground into a powder form with diameters < 150 μm to ensure homogeneity. One to 2 mg of the powdered sample was placed into stannum cups for carbon isotope analysis. The carbon isotopic compositions of *Hydrilla verticillata* samples were determined using an elemental analyzer coupled to an isotope-ratio mass spectrometer (EA-IRMS). The isotopic

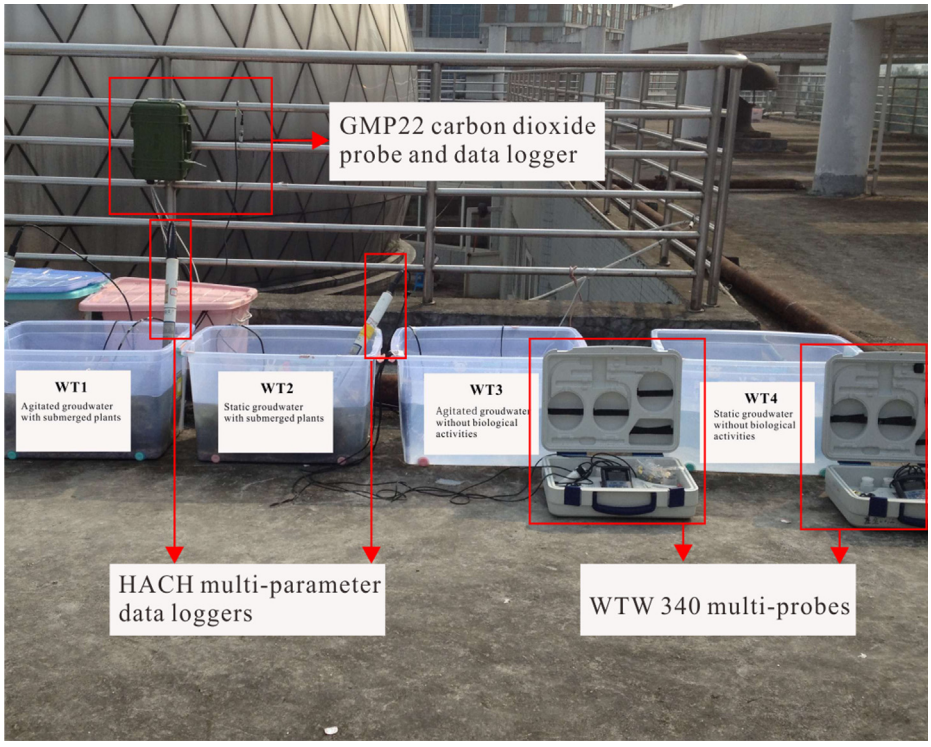

Fig. 1. Experimental set-up.

Table 3
The correlations between Ca^{2+} and SpC, HCO_3^- and SpC.

Reactor ID	WT1	WT2	WT3	WT4
[Ca^{2+}]	0.26 SpC −48.44	0.21 SpC −3.44	0.3 SpC −78.58	0.37 SpC −120.69
Correlation coefficient	r^2 = 0.99	r^2 = 0.93	r^2 = 0.99	r^2 = 0.97
[HCO_3]	0.85 SpC −189.04	0.98 SpC −696.87	0.8 SpC −169.75	0.95 SpC −287.38
Correlation coefficient	r^2 = 0.99	r^2 = 0.96	r^2 = 0.97	r^2 = 0.96

The brackets denote concentrations in mg/L and SpC is specific conductivity in μS/cm at 25 °C.

analyses were conducted in the Environmental Stable Isotope Laboratory of the Chinese Academy of Agricultural Sciences. Stable carbon isotope results, $\delta^{13}C$, are expressed in the usual delta-notation per mil (‰) deviation from the standard Vienna Pee Dee Belemnite (V-PDB). The overall experimental accuracy for $\delta^{13}C$ measurements was ± 0.2‰.

Meteorological data were recorded from a BS28-VP2 field weather station located at the experimental site. Parameters were measured at 15 min interval, including air temperature, solar radiation and evaporation rate. The resolutions of the measurements were 0.5 °C, 5% and 0.25 mm, respectively.

3. Data processing and analysis

3.1. Preprocessing

Since Ca^{2+} and HCO_3^- are the main ions in karst waters, the time series of Ca^{2+} and HCO_3^- concentrations were calculated from the linear relationship between the in-situ titration data and logged data of SpC (Table 3). The DIC concentrations were calculated from the time series of HCO_3^- (CO_3^{2-}) concentrations and logged data of pCO_2.

3.2. Determining DIC loss by CO_2 evasion

Carbon dioxide fluxes across the water–air interface were calculated using a molecular diffusion model (Raymond et al., 2012):

$$Fa = k* (pCO_{2water} - pCO_{2air}) \quad (2)$$

where F is the CO_2 evasion flux (mg/m^2·15 min) between water and air, k is the gas transfer velocity (cm/15 min), $pCO_{2water} - pCO_{2air}$ is the CO_2 concentration gradient between the water and air, in ppmv. The value of k is calculated using the temperature-dependent Schmidt number (Sc_T) for fresh water (Raymond et al., 2012).

3.3. Determining changes in DIC concentrations from calcite

Carbonate precipitation decreases Ca^{2+} and HCO_3^- concentrations by a ratio of 1:2 mol, and simultaneously releases 1 mol of $CO_{2(aq)}$ into solution, and conversely, carbonate dissolution increases Ca^{2+} and HCO_3^- concentrations by a ratio of 1: 2 mol, and remove 1 mol of $CO_{2(aq)}$ from the solution. Thus, the DIC loss by calcite precipitation or gain by calcite dissolution were calculated from the changes in Ca^{2+} concentrations and molar ratio between Ca^{2+} and HCO_3^- concentrations.

3.4. Determining changes in DIC from the metabolism of Hydrilla verticillata

The biologically-generated DIC was obtained from the gross primary productivity (GPP) and respiration rates (R) through variations in DO concentrations (Hotchkiss and Hall, 2014; Tobias et al., 2007). GPP and R were calculated using a one-station, open-channel metabolism model (Odum, 1956), where the change in DO concentrations between measurement intervals (t and t − 1) are a function of R, GPP, air–water gas exchange, and the change in time between measurements (Δt). During this study, Δt = 15 min.

$$O_{2(t)} = O_{2(t-1)} + ((GPP + R) + K_{O_2}(O_{2sat_{(t-1)}} - O_{2(t-1)}))\Delta t \quad (3)$$

Where R and GPP are O_2 consumption and production rates. For O_2 production, GPP and R values are positive rates, and for O_2 consumption, GPP and R values are negative rates respectively, expressed in mg O_2 min^{-1}; K_{O_2} is the O_2 gas–water exchange rate, determined from the slope of the line relating the change in DO per 15 min intervals and the DO saturation deficit; $O_{2sat_{(t)}}$(mg O_2) is the saturation concentration of DO, calculated from water temperature (Gilcreas, 1966); R is the estimated night-time DO variations caused by the respiration of aquatic plants based on a temperature-driven O_2 metabolism model according to Eq. (4).

$$R = R_{night} \times 1.047^{(T - T_{average})} \quad (4)$$

where R_{night} is average respiration rate at night; T and $T_{average}$ are the observed water temperature and the average value of water temperature (°C), respectively. The GPP can be calculated from the mass balance of DO concentrations. The DIC affected by the metabolism of *Hydrilla verticillata* can be estimated based on C:O_2 molar stoichiometry (1:1) (del Giorgio and Williams, 2005).

3.5. Estimated magnitudes of $\delta^{13}C_{DIC}$ variations

The contributions of biological, chemical and physical processes to variations in $\delta^{13}C_{DIC}$ were calculated using a time-stepping chemical/isotope (^{12}C and ^{13}C) mass balance model (Tobias and Böhlke, 2011) based on the DIC loss/gain. The model requires (1) the initial $\delta^{13}C$ values of the DIC from the karst spring water (Table 2), *Hydrilla verticillata* and atmospheric CO_2 (Table 4); (2) the isotope fractionation factors α, (defined as Ra/Rb, where R is the isotopic ratio of $^{13}C/^{12}C$ between $C_{species}$ of air–water exchange ($CO_{2(aq)}/CO_{2(gas)}$ at equilibrium) (Zhang et al., 1995). The fractionation factor used for air–water exchange (for $CO_{2(aq)}$–$CO_{2(gas)}$ equilibrium) and gas dissolution are 0.9989 ± 0.0002 and 1.00118 ± 0.0004 at 25 °C (Zhang et al., 1995), for carbonate precipitation ($HCO_3^-/CaCO_3$) is 1.00185 ± 0.0001 (Turner, 1982), for photosynthesis and respiration by *Hydrilla verticillata* assumed to be constants at 0.9830 (Mook, 2006; Bade et al., 2006) and 1.0000 (assuming no fractionation during the respiration of Org C to CO_2), respectively. The $\delta^{13}C_{DIC}$ values were calculated from the modeled ^{12}C and ^{13}C molar concentrations according to the relation:

$$\delta^{13}C_{DIC} = (13\,C/12\,C \cdot 89.45 - 1) \quad (5)$$

where 89.45 is the molar ratio of $^{12}C/^{13}C$ in the VPDB isotopic reference (Coplen et al., 2002).

Table 4
Average initial $\delta^{13}C$ values for the DIC model.

Source	$\delta^{13}C$ (‰)
Hydrilla verticillata (n = 8)	−19.3 (varying from −17.9‰ to −20.8‰)
atmospheric CO_2 (n = 14)	−9.9 (varying from −8.0‰ to −11.9‰)

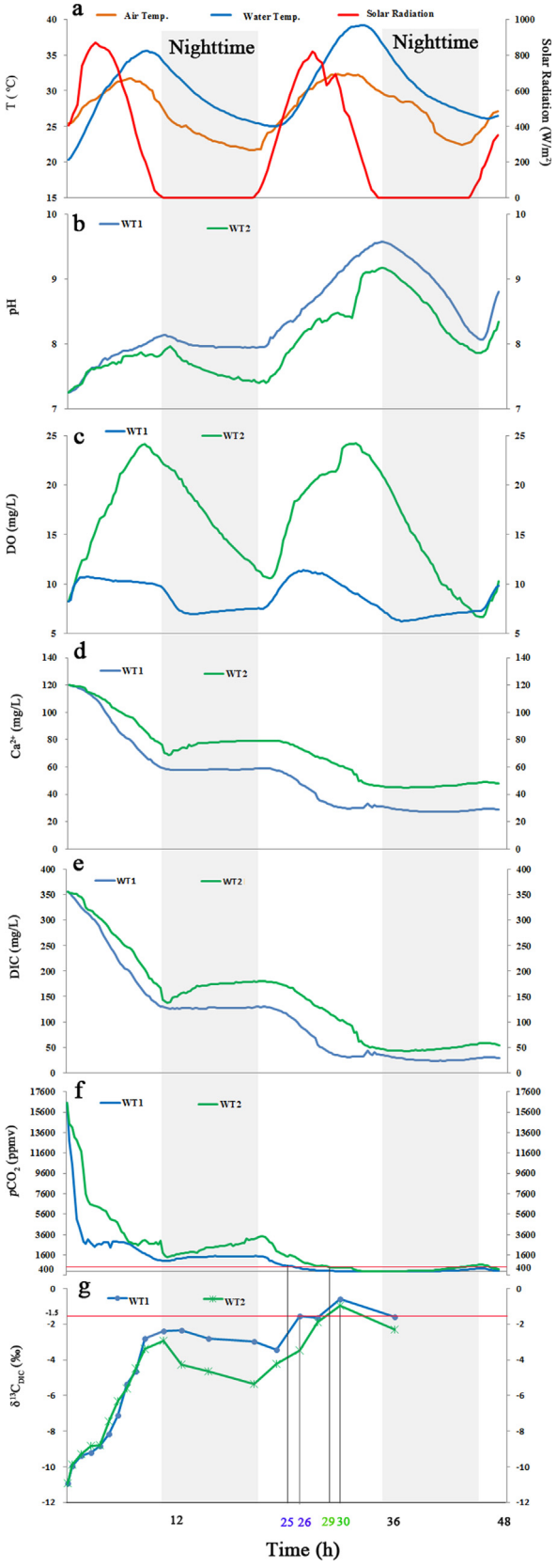

Fig. 2. The temporal variations of the physico-chemical parameters of WT1 (agitated karst spring-water with *Hydrilla verticillata*) and WT2 (static karst spring-water with *Hydrilla verticillata*). White areas represent daytime and Gary areas represent nighttime which are determined from the amount of solar radiation. The horizontal red lines of p_{CO_2} and $\delta^{13}C_{DIC}$ represent chemical and isotopic equilibrium with atmospheric CO_2 (410 ppmv and −1.5‰, respectively). The vertical lines represent the time when p_{CO_2} and $\delta^{13}C_{DIC}$ reached chemical and isotopic equilibrium with atmospheric CO_2, respectively. (For interpretation of the references to colour in this figure legend, the reader is referred to the web version of this article.)

3.6. Equilibrium values of DIC and $\delta^{13}C_{DIC}$

For the duration of the experiments, atmospheric pCO_2 varied between 350 ppmv and 500 ppmv with a mean value of 410 ppmv (Table 2), and $\delta^{13}C_{CO2}$ varied between −8.0‰ and −11.9‰ with a mean value of −9.9‰ (Table 4). The stable carbon isotope fractionation between DIC and $CO_{2(g)}$ is about +8.4‰ at 25 °C (Zhang et al., 1995). Therefore, the pCO_2 and $\delta^{13}C_{DIC}$ in karst waters that achieve chemical and isotopic equilibrium with atmospheric $CO_{2(g)}$ will be around 410 ppmv and −1.5‰ (+0.4‰ to −3.5‰), respectively.

4. Results

4.1. Temporal variations of physico-chemical parameters and $\delta^{13}C_{DIC}$ in agitated karst spring-waters with Hydrilla verticillata: WT1

The pH in WT1 (Fig. 2b) showed a small diel variation, characterized by daytime increases and nighttime decreases. During the first 2 h of the experiment, pH increased rapidly from 7.25 to 8.00, followed by a slower increase to 8.15 before decreasing to 7.95 overnight. The following daytime, pH increased again to 9.58, followed by a steady decreased to 8.07 by night. The overall pH increase was by 2.3 pH units, and the range was 1.0 pH unit during day 1 and 1.5 pH units during day 2, respectively.

The DO concentrations in WT1 (Fig. 2c) showed a diel variation with an amplitude of about 5.2 mg/L. DO steadily increased to a peak of 11.4 mg/L during the day and then decreased gently to a low of 6.2 mg/L by nighttime.

The Ca^{2+} and DIC concentrations in WTI (Fig. 2d and e) decreased steeply during the day and slightly flattened during the night. Ca^{2+} decreased from a high of 120 mg/L to 58 mg/L during the first day, and stabilized around a final low of 27 mg/L by the end of the experiment. DIC decreased from 356 mg/L to 125 mg/L during the first day, and stabilized around a low of 25 mg/L by the end of the experiment.

The pCO_2 in WTI (Fig. 2f) showed a similar trend to Ca^{2+} and DIC concentrations, but differed in the steepness of the decreases during the daytime and the sharp transitions between day and night during the first 24 h. During the first 2 h, pCO_2 decreased steeply from 16,500 ppmv to 3000 ppmv, then gradually to 1000 ppmv over the next 11 h. During the nighttime a slight steady increase to 1500 ppmv occurred. During the next daytime, the pCO_2 again decreased sharply to a low of 410 ppmv and then gradually decreased to ~0 ppmv till the end of the experiment.

As shown in Fig. 2g, the $\delta^{13}C_{DIC}$ in WT1 generally increased. The $\delta^{13}C_{DIC}$ in WT1 was enriched by +8.5‰ (−10.9‰ to −2.4‰) during the first 10 h, and was slightly depleted by −1.1‰ (−2.4 to −3.5‰) overnight. The following day, enrichment of the $\delta^{13}C_{DIC}$ in WT1 occurred by +3.1‰ (−3.5‰ to −0.6‰) before slightly decreasing at night.

4.2. Temporal variations of physico-chemical parameters and $\delta^{13}C_{DIC}$ in static karst spring-water with Hydrilla verticillata: WT2

The pH in WT2 sample (Fig. 2b) showed a similar variation to WT1, but was characterized by lower pH values. The pH increased from 7.25 to 7.96 during the first day, and then decreased to 7.40 at night. The pH increased rapidly to 9.17 during the following daytime, and then decreased to 7.86 at night.

The DO concentrations in WT2 (Fig. 2c) also showed a marked diel variation of about 13.6 mg/L that peaked at 24.0 mg/L during the day and dropped to a low of 10.6 mg/L overnight till the next morning. Unlike WT1, sharp peaks and troughs observed for DO values lasted for about 1 h.

The Ca^{2+} and DIC concentrations in WT2 (Fig. 2d and e) showed similar variations to those observe for WT1 with generally higher values. They showed a notable decrease during the daytime and slight increases at nighttime. During the first day, Ca^{2+} and DIC decreased steeply from 120 mg/L to 70 mg/L, and 356 mg/L to 140 mg/L during the day, and then slightly increased to 80 mg/L and 180 mg/L overnight, respectively. The next day, Ca^{2+} and DIC gradually decreased to 45 mg/L and 42 mg/L during the daytime, and then stabilized around a low of 48 mg/L and 58 mg/L to the end of the experiment, respectively.

The pCO_2 for WT2 (Fig. 2f) also generally decreased, with small diel variations. The pCO_2 values decreased steeply from 16,500 ppmv down to 3000 ppmv during the first 7 h, and then gradually to 1500 ppmv over the next 5 h before slightly increasing to 3500 ppmv overnight. In the following day, the pCO_2 values sharply decreased to 410 ppmv by 29 h and then gradually decreased to ~0 ppmv to the end of the experiment.

The $\delta^{13}C_{DIC}$ of WT2 (Fig. 2g) also generally increased. The $\delta^{13}C_{DIC}$ had slightly higher during the first 10 h and lower values afterwards compared to WTI. During the first day, the $\delta^{13}C_{DIC}$ of WT2 was enriched by +8.0‰, (−10.9‰ to −2.9‰) during the daytime, and was slightly depleted by −2.5‰, (−2.5‰ −5.4‰) during the nighttime. The next day, the $\delta^{13}C_{DIC}$ was enriched by +4.4‰ (−5.4‰ to −1.0‰) during the day and then dropped to −2.3‰ at night.

4.3. Temporal variations of physico-chemical parameters and $\delta^{13}C_{DIC}$ in agitated karst spring-water without Hydrilla verticillata: WT3

The pH in WT3 (Fig. 3b), generally increased to the end of the experiment with an overall increase of 1.3 pH units. During the first 12 h, pH steeply increased from 7.25 to 8.10, followed by a gradual increase to 8.60 during the rest of the experiment.

The DO concentrations in WT3 (Fig. 3c) showed symmetrical diel variations but inversely in phase with water temperature, characterized by an increase of about 1 mg/L in the mornings and evenings. The peak concentrations were around 8 mg/L and troughs were above 6.5 mg/L.

The Ca^{2+} and DIC concentrations in WT3 (Fig. 3d and 3e) declined steadily from 120 mg/L to 50 mg/L, and 356 mg/L to 110 mg/L to the end of the experiment, respectively.

The pCO_2 in WT3 (Fig. 3f) showed a similar but more abrupt trend of decline compared to Ca^{2+} and DIC. During the first 12 h, the pCO_2 decreased steeply from 16,500 ppmv to 2000 ppmv. During the night, the pCO_2 continued to decline gradually to 410 ppmv after 70 h and then slowly to 300 ppmv to the end of the experiment.

The $\delta^{13}C_{DIC}$ of WT3 (Fig. 3g) showed a different temporal pattern when compared to WT1 and WT2. The $\delta^{13}C_{DIC}$ of WT3 was rapidly enriched by +7.4‰ (from −10.9‰ to −3.5‰) at the first 36 h, followed by a more gradual enrichment phase to −1.5‰.

4.4. Temporal variations of physico-chemical parameters and $\delta^{13}C_{DIC}$ in static karst spring-water without Hydrilla verticillata: WT4

The pH in WT4 (Fig. 4b) also generally increased to the end of the experiment with an overall increase of 1.1 pH units. The pH increased gradually from 7.25 to 8.00 during the first 36 h, and then increased more slowly to 8.45 after 168 h and then fluctuated at 8.40 till the end of the experiment.

DO concentrations in WT4 (Fig. 4c) showed a cyclical diel pattern that varied out of phase with water temperature. The DO cycles had increases of about 1 mg/L with the maxima in the mornings and minima in the evenings. The diel pattern shows symmetry with sharp minimum and maximum peaks and varied between 6.5 mg/L and 8.0 mg/L.

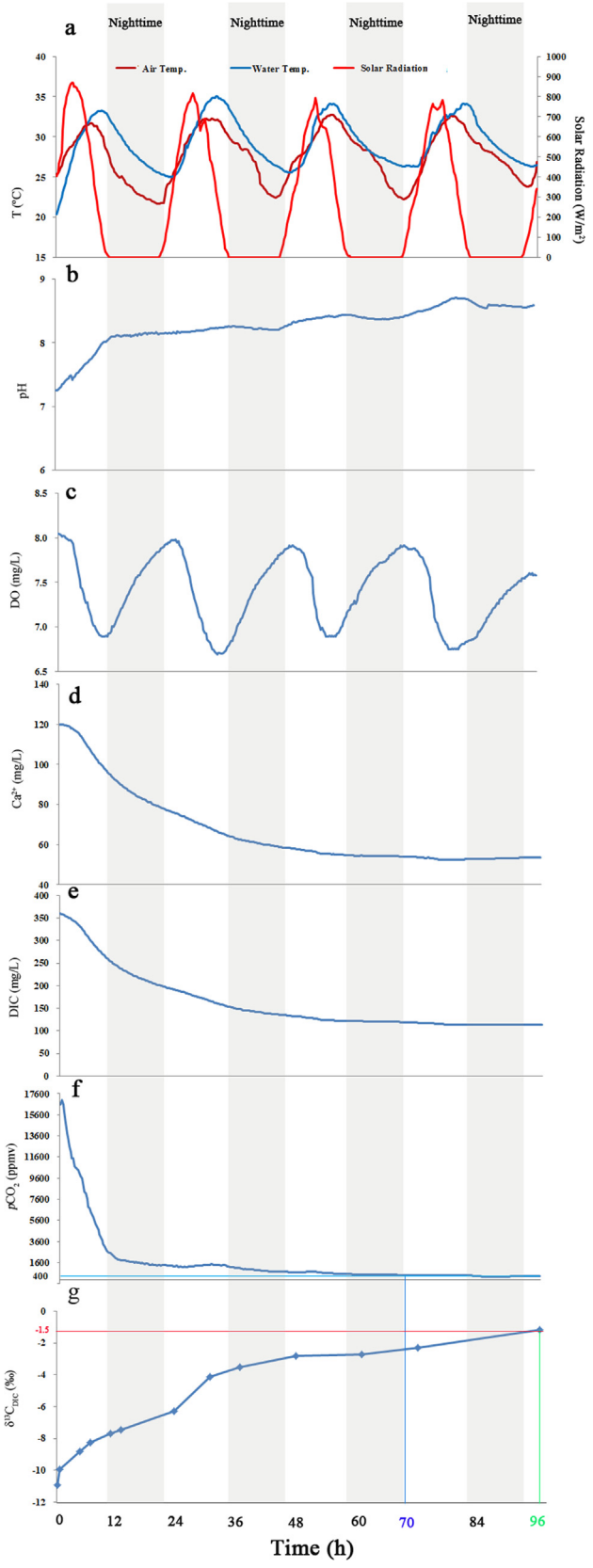

Fig. 3. The temporal variations of the physico-chemical parameters of WT3 (agitated karst spring-water without *Hydrilla verticillata*). The horizontal lines of pCO_2 and $\delta^{13}C_{DIC}$ represent chemical and isotopic equilibrium with atmospheric CO_2 (410 ppmv and −1.5‰, respectively). The vertical lines represent the time when pCO_2 and $\delta^{13}C_{DIC}$ reached chemical and isotopic equilibrium with atmospheric CO_2, respectively.

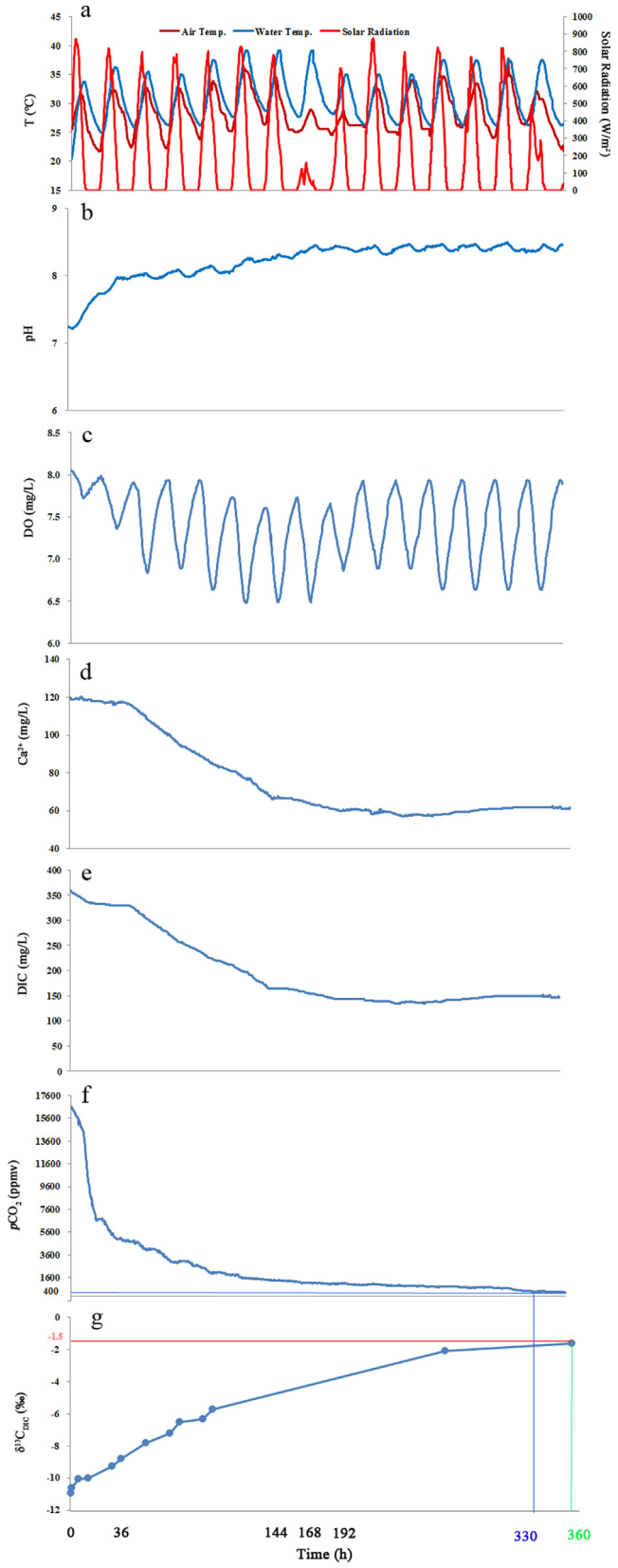

Fig. 4. The temporal variations of the physico-chemical parameters of WT4 (static karst spring-water without *Hydrilla verticillata*). The horizontal lines of p_{CO_2} and $\delta^{13}C_{DIC}$ represent chemical and isotopic equilibrium with atmospheric CO_2 (410 ppmv and −1.5‰, respectively). The vertical lines represent the time when p_{CO_2} and $\delta^{13}C_{DIC}$ reached chemical and isotopic equilibrium with atmospheric CO_2, respectively.

The Ca^{2+} and DIC concentrations in WT4 (Fig. 4d and e) generally decreased over time. During the first 36 h, the Ca^{2+} and DIC concentrations remained near stable, followed by a steep decline to about 144 h before slightly steadying to the end of the experiment. Ca^{2+} decreased from 117 mg/L to 60 mg/L and DIC decreased from 330 mg/L to 145 mg/L and then remained more or less stable until the end of experiment.

The pCO_2 in WT4 (Fig. 4f) decreased steeply from 16,500 ppmv to 5000 ppmv during the first 36 h, and then gradually to 1400 ppmv after 144 h. The *p*CO2 continued to decrease slowly to 1000 ppmv by the 192 h, and then to 410 ppmv after 330 h and then stabilized to the end of the experiment.

The $\delta^{13}C_{DIC}$ of WT4 (Fig. 4g) showed similar variation as WT3 (Fig. 3g). The $\delta^{13}C_{DIC}$ increased with slight enrichment of + 0.9‰ (from −10.9‰ to −10.0‰) during the first 12 h, followed by significant enrichment of +7.9‰ (from −10.0‰ to −2.1‰) during the next 256 h. By the end of the experiment, gradual enrichment continued to −1.5‰.

5. Discussion

5.1. Chemical and isotopic behavior of DIC in karst spring-waters exposed to the atmosphere

The DIC concentrations and $\delta^{13}C_{DIC}$ in treated karst spring-waters with different hydro-biological conditions, exposed to the same atmosphere, exhibit different temporal, chemical and isotopic behaviors (Figs. 5 and 6, and Table S1). Although the DIC concentrations and $\delta^{13}C_{DIC}$ in all karst spring-waters reached chemical and isotopic equilibrium with atmospheric CO_2 (Fig. 2e, 2 g, 3e, 3 g, 4e and 4 g), DIC loss and $\delta^{13}C_{DIC}$ enrichment are faster in waters that contained *Hydrilla verticillata* (WT1 and WT2) than in waters without *Hydrilla verticillata* (WT3 and WT4). DIC loss and $\delta^{13}C_{DIC}$ enrichment are faster in agitated waters than in static waters (WT1 vs. WT2, and WT3 vs. WT4). It took 25 h and 26 h for the agitated water with *Hydrilla verticillata* (WT1), and 29 h and 30 h for the static water with *Hydrilla verticillata* (WT2), to reach chemical and isotopic equilibrium with atmospheric CO_2, respectively. Meanwhile, it took more time, 70 h and 96 h for the agitated water without *Hydrilla verticillata* (WT3), and 330 h and 360 h for the static water without *Hydrilla verticillata* (WT4), to reach chemical and isotopic equilibrium with atmospheric CO_2, respectively. Since all the waters were obtained from the same karst spring source, and had similar initial DIC concentrations and $\delta^{13}C_{DIC}$ values, and were all exposed to the same laboratory atmosphere, the different temporal response, and chemical and isotopic behaviors of the waters as they attained equilibrium could be attributed to differences in hydro-biological conditions of the treated waters. Thus, such significant differences in the temporal evolution of DIC and $\delta^{13}C_{DIC}$ in karst spring-waters exposed to the atmosphere is primarily related to the effects of the aquatic plants, and also of the water agitation. With these observations, we show that by evaluating the effects of different processes (physical, chemical and biological) under different hydrological conditions on the temporal evolution of DIC and $\delta^{13}C_{DIC}$, greater insights into how and why different Karst spring-waters exhibit different chemical and isotopic behaviors are gained.

5.2. DIC-$\delta^{13}C_{DIC}$ evolution in karst spring-waters with/without aquatic plants: metabolic process vs. physical process vs. chemical process

Fig. 7 shows that as waters evolved to chemical equilibrium with atmospheric CO_2, for the waters with aquatic plants (WT1 and WT2), the DIC evolution is primarily controlled by metabolic processes (photosynthesis and respiration) of *Hydrilla verticillata*. During metabolism, the DIC loss by *Hydrilla verticillata* was 200 mmol (accounting for 42%) and 210 mmol (accounting for 44%) in WT1 and WT2, respectively, of which 225 mmol and 225 mmol of DIC was used for

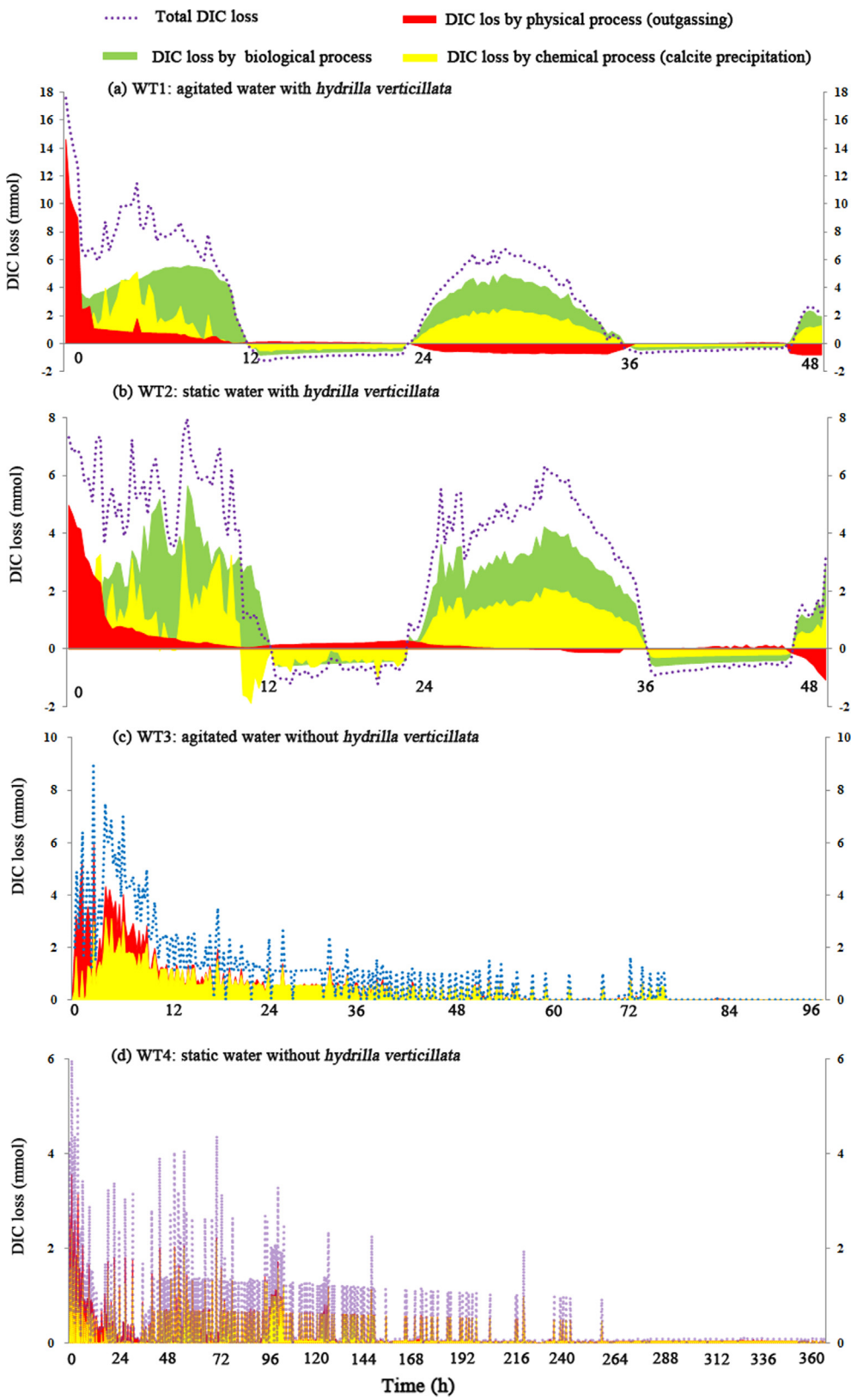

Fig. 5. Calculated results of total DIC loss and DIC loss by three different processes (CO_2 evasion, calcite precipitation and metabolism by *Hydrilla verticillata*) by 15 min intervals over time. The positive values represent DIC loss by photosynthesis, calcite precipitation and CO_2 evasion. The negative values represent DIC gain by respiration, carbonate dissolution and CO_2 absorption.

photosynthesis, while 25 mmol and 15 mmol DIC were produced during the respiration of *Hydrilla verticillata* in WT1 and WT2, respectively. The secondary control on the DIC evolution as the waters evolved to chemical equilibrium with atmospheric CO_2 is calcite precipitation/dissolution, where 95 mmol and 100 mmol DIC were lost by calcite precipitation, while 15 mmol and 25 mmol were produced by calcite

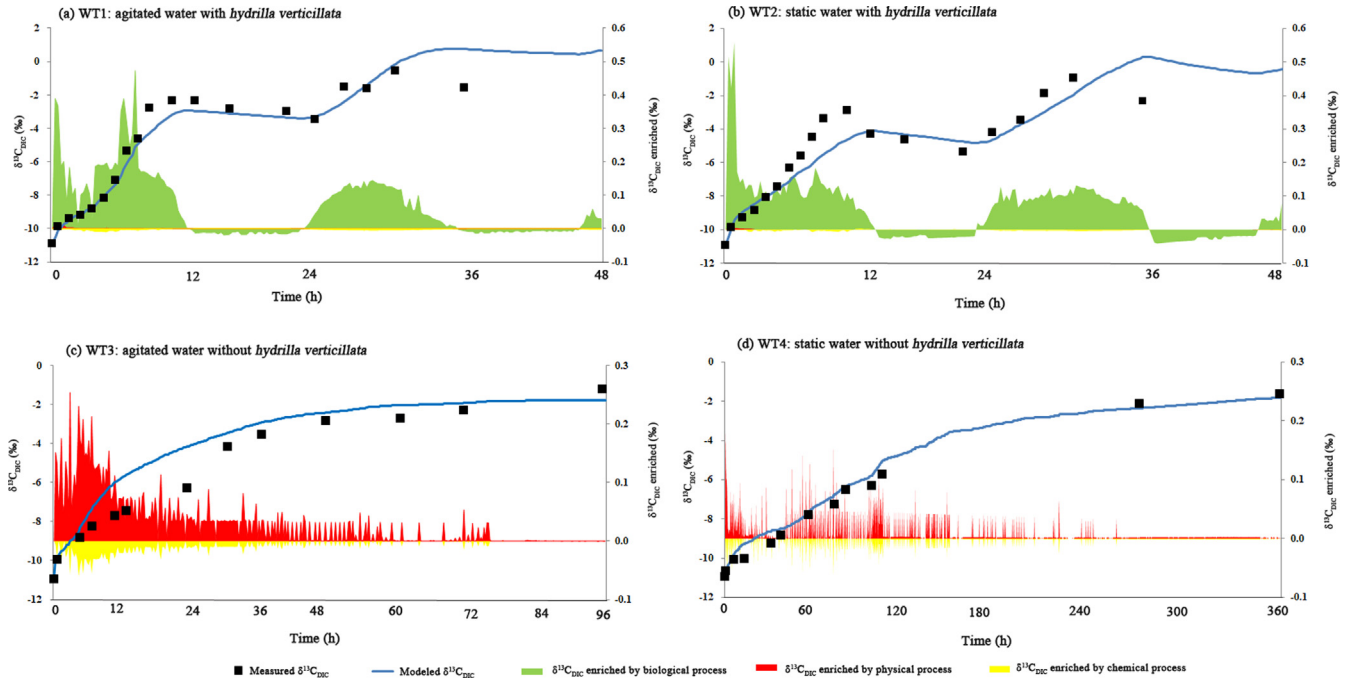

Fig. 6. The measured and modeled values of $\delta^{13}C_{DIC}$, and ^{13}C fractionation enrichment due to physical, chemical and biological processes.

dissolution in WT1 and WT2, respectively. The third control on DIC evolution is CO_2 outgassing, where 75 mmol and 55 mmol CO_2 was released to the atmosphere as the waters evolved to chemical equilibrium with atmospheric CO_2 in WT1 and WT2, respectively. In contrast, as the waters without aquatic plants evolved to chemical equilibrium with atmospheric CO_2, the DIC evolution was primarily controlled by CO_2 outgassing, where 210 mmol (accounting for 44%) and 240 mmol (accounting for 50%) of CO_2 were released to the atmosphere from WT3 and WT4, respectively. The DIC evolution in these waters without aquatic plants was secondly controlled by calcite precipitation, where 150 mmol and 190 mmol of DIC were lost from WT3 and WT4, respectively, as the waters evolved to chemical equilibrium with atmospheric CO_2. Thus, the sharp decrease in DIC concentrations observed in WT1 and WT2 is primarily caused by the photosynthesis of *Hydrilla verticillata,* while the gentler loss in DIC observed in WT3 and WT4 is caused by CO_2 outgassing and calcite precipitation.

Similarly to DIC evolution, as shown in Fig. 7 and Table S1, for Karst spring-waters with aquatic plants (WT1 and WT2), the $\delta^{13}C_{DIC}$ evolution is almost entirely controlled by the metabolic activities (photosynthesis and respiration) of *Hydrilla verticillata*. As a result, the $\delta^{13}C_{DIC}$ was enriched by 12.65‰ and 12.47‰ during photosynthesis and depleted by −0.82‰ and −1.78‰ during respiration in WT1 and WT2, respectively. Calcite precipitation/dissolution and CO_2 outgassing show negligible effects on the $\delta^{13}C_{DIC}$ evolution in these waters (WT1 and WT2). In contrast, for waters without aquatic plants, as the waters evolved to isotopic equilibrium with atmospheric CO_2, the $\delta^{13}C_{DIC}$ increased by 11.90‰ and 14.20‰ as a result of CO_2 outgassing, and decreased by 2.80‰ and 5.10‰ due to calcite precipitation in WT3 and WT4 respectively. Thus, the observed sharp increase in $\delta^{13}C_{DIC}$ in WT1 and WT2 waters is primarily resulted from the photosynthesis of *Hydrilla verticillata*, while the slower increase in $\delta^{13}C_{DIC}$ in WT3 and WT4 is entirely caused by CO_2 outgassing.

5.3. DIC-$\delta^{13}C_{DIC}$ evolution in the agitated/static karst spring-waters

The results in Fig. 7 and Table S1, show that not only are there differences in the rate of DIC loss from the waters subject to different bio-chemical treatments, there is also a significant difference in the amount of DIC loss due to different physical treatment either by agitation or static.

For agitated waters (WT1 vs. WT2), the water with aquatic plants (WT1), lost 75 mmol DIC (15% of the total DIC), 80 mmol DIC (17% of the total DIC) and 200 mmol DIC (42% of the total DIC) by outgassing, calcite precipitation and photosynthesis, respectively, within 25 h, while the static water (WT2) treated with the same aquatic plants lost 55 mmol DIC (11% of the total DIC), 75 mmol DIC (16% of the total DIC) and 210 mmol DIC (44% of the total DIC) by outgassing, calcite precipitation and photosynthesis within 29 h, respectively. In other words, our results suggest that the average rate of DIC loss by the CO_2 evasion, calcite precipitation and photosynthesis is about 3.0 mmol/h, 3.2 mmol/h and 8.0 mmol/h, respectively, for agitated (turbulent) Karst spring-water with aquatic plants, and 1.9 mmol/h, 2.6 mmol/h and 7.2 mmol/h, respectively, for static (lamina) Karst spring-water with the same aquatic plants.

Regarding waters without aquatic plants, (WT3 vs. WT4), for the agitated water without the aquatic plants (WT3), 210 mmol DIC (44% of the total DIC) and 150 mmol DIC (31% of the total DIC) was lost to the atmosphere by outgassing and lost by calcite precipitation within 70 h, respectively, while in the static water without aquatic plants 240 mmol DIC (50% of the total DIC) and 190 mmol DIC (40% of the total DIC) (WT4) was lost to the atmosphere by outgassing and by calcite precipitation after 330 h, respectively. In other words, the average rate of DIC loss by CO_2 evasion and calcite precipitation from agitated karst spring-water without aquatic plants, is about 3.0 mmol/h and 2.1 mmol/h, respectively, while the average rate of DIC loss by CO_2 evasion is 0.7 mmol/h and by calcite precipitation is 0.6 mmol/h in static karst spring-water without aquatic plants. These results suggest that the agitation (turbulence) of water accelerates CO_2 evasion, calcite precipitation and photosynthesis of aquatic plants (*Hydrilla verticillata)*.

However, as shown in Table S1 and Fig. 7, although no obvious differences appear in the overall $\delta^{13}C_{DIC}$ enrichment for the agitated and static karst spring-waters with/without aquatic plants, there are marked differences in the timing of when the karst spring-waters evolved to isotopic equilibrium with atmospheric CO_2 in the agitated and static karst spring-waters. The $\delta^{13}C_{DIC}$ enrichment is faster in the agitated waters than that in the static waters, indicating that the agitation (turbulence) of water may accelerate $\delta^{13}C_{DIC}$ enrichment.

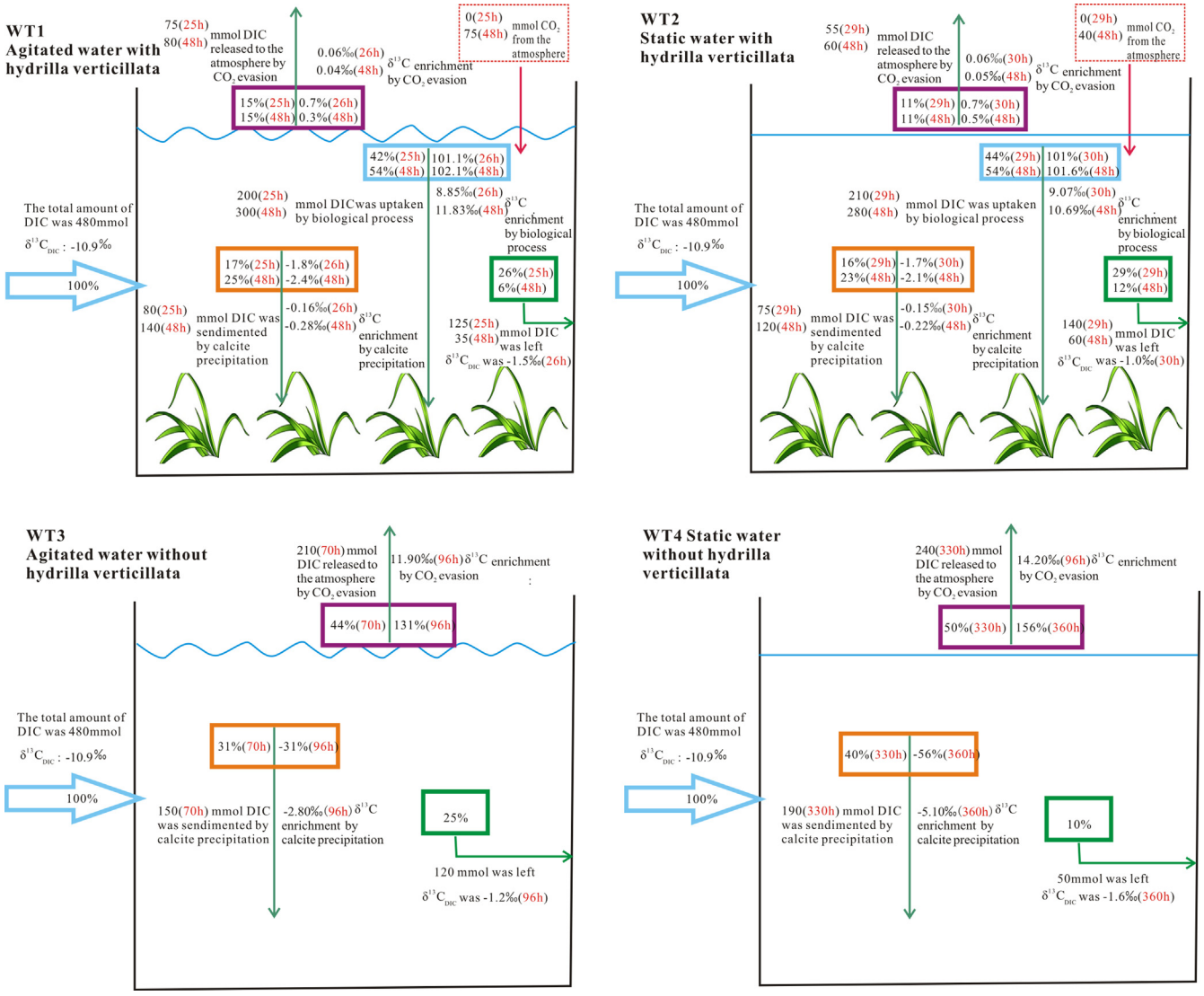

Fig. 7. Schematic illustration of the evolution of DIC and $\delta^{13}C_{DIC}$ in WT1, WT2, WT3 and WT4.

6. Implications

Our results show that DIC produced from carbonate weathering can be used by aquatic organisms thereby converting it into OC. This means that the view of carbon shifts that exclude sequestration during the transformation of weathered carbonate rock deposits (Curl, 2012) could be revisited in order to factor in the proportion of DIC from the weathered carbonate that is converted by aquatic plants through photosynthesis into organic carbon for possible long-term sequestration by aquatic organisms rather than being released to the atmosphere as CO_2 in continental surface water systems or oceans.

Furthermore, as shown in Fig. 7, the significant flux of CO_2 from the atmosphere to the karst spring-waters after they attain chemical equilibrium with atmospheric CO_2, suggest that intense aquatic photosynthetic activities in continental surface water systems could play an important role as a natural carbon sink, drawing CO_2 directly from the atmosphere when there is not enough DIC in the waters (rivers and streams) to maintain the normal metabolic rates of the aquatic organisms.

7. Conclusion

At the laboratory scale, the temporal evolutions of DIC and $\delta^{13}C_{DIC}$ in karst spring-waters with high pCO_2 exposed to atmospheric CO_2 under agitated and static conditions with/without aquatic plants were quantitatively assessed. The controls on DIC and $\delta^{13}C_{DIC}$ of the karst spring-waters during evolution to equilibrium with atmospheric CO_2 were deciphered. Results of the temporal behavior of DIC and $\delta^{13}C_{DIC}$ observed from the laboratory experiments could be applied to characterize carbon evolution in carbonate-rich surface waters (e.g., streams, lakes and reservoirs) evolving and interacting with the atmosphere.

DIC evolution appears to be mainly controlled by the metabolism of aquatic plants (< 40%), while calcite precipitation/dissolution and CO_2 outgassing show little effects on the DIC evolution in the karst spring-waters with aquatic plants (< 20%). The $\delta^{13}C_{DIC}$ evolution is also mainly controlled by the metabolism of the aquatic plants, while calcite precipitation/dissolution and CO_2 outgassing have a lesser effect on the $\delta^{13}C_{DIC}$ evolution in the karst spring-waters with aquatic plants.

Declaration of Competing Interest

The authors declare that they have no known competing financial interests or personal relationships that could have appeared to influence the work reported in this paper.

Acknowledgement

This research was supported by the national key research and developmental program of China (2016YFC0502306), Chongqing Municipal Science and Technology Commission Fellowship Fund (CSTC2017jcyj-ysxX0004) and the National Natural Science Foundation of China (41472321). Special thanks are given to two anonymous reviewers, and Prof. Huaming whose constructive comments and suggestions have greatly improved this manuscript.

Appendix A. Supplementary data

Supplementary data to this article can be found online at https://doi.org/10.1016/j.jhydrol.2019.124294.

References

Abongwa, P.T., Atekwana, E.A., 2013. Assessing the temporal evolution of dissolved inorganic carbon in waters exposed to atmospheric CO_2(g): a laboratory approach. J. Hydrol. 505 (8), 250–265.

Abongwa, P.T., Atekwana, E.A., 2015. Controls on the chemical and isotopic composition of carbonate springs during evolution to saturation with respect to calcite. Chem. Geol. 404, 136–149.

Atekwana, E.A., Krishnamurthy, R.V., 1998. Seasonal variations of dissolved inorganic carbon and δ^{13}C of surface waters: application of a modified gas evolution technique. J. Hydrol. 205, 265–278.

Aufdenkampe, A.K., Mayorga, E., Raymond, P.A., Melack, J.M., Doney, S.C., Alin, S.R., Aalto, R.E., Yoo, K., 2011. Riverine coupling of biogeochemical cycles between land, oceans, and atmosphere. Front. Ecol. Environ. 9 (1), 53–60.

Bade, D.L., Pace, M.L., Cole, J.J., Carpenter, S.R., 2006. Can algal photosynthetic inorganic carbon isotope fractionation be predicted in lakes using existing models? Aquat. Sci. 68 (2), 142–153.

Battin, T.J., Luyssaert, S., Kaplan, L.A., Aufdenkampe, A.K., Richter, A., Tranvik, L.J., 2009. The boundless carbon cycle. Nat. Geosci. 2 (9), 598–600.

Chen, B., Ynag, R., Liu, Z., Sun, H., Yan, H., Zeng, Q., Zeng, S., Zeng, C., Zhao, M., 2017. Coupled control of land uses and aquatic biological processes on the diurnal hydrochemical variations in the five ponds at the Shawan Karst Test Site, China: implications for the carbonate weathering-related carbon sink. Chem. Geol. 456, 58–71.

Clark, I.D., Fritz, P., 1997. Environmental Isotopes in Hydrogeology. CRC Press, pp. 352.

Cole, J.J., Prairie, Y.T., Caraco, N.F., McDowell, W.H., Tranvik, L.J., Striegl, R.G., Duarte, C.M., Kortelainen, P., Downing, J.A., Middelburg, J.J., Melack, J., 2007. Plumbing the global carbon cycle: Integrating inland waters into the terrestrial carbon budget. Ecosystems 10 (1), 171–184.

Coplen, T.B., Hopple, J.A., Böhlke, J.K., Peiser, H.S., Rieder, S.E., Krouse, H.R., Rosman, K.J.R., Ding, T., Vocke Jr., R.D., Révész, K.M., Lamberty, A., Taylor, P.D.P., De Bièvre, P., 2002. Compilation of minimum and maximum isotope ratios of selected elements in naturally occurring terrestrial materials and reagents. U.S. Geological Survey Water-Resources Investigations Report 01-4222. 98 pp.

Curl, R., 2012. Carbon shifted but not sequestered. Science 335 (6069), 655.

de Montety, V., Martin, J.B., Cohen, M.J., Foster, C., Kurz, M.J., 2011. Influence of diel biogeochemical cycles on carbonate equilibrium in a karst river. Chem. Geol. 283, 31–43.

del Giorgio, P.A., Williams, P.B., 2005. Respiration in Aquatic Ecosystems. Oxford University Press, New York, pp. 315.

Dreybrodt, W., Buhmann, D., Michaelis, J., Usdowski, E., 1992. Geochemically controlled calcite precipitation by CO_2 outgassing: field measurements of precipitation rates in comparison to theoretical predictions. Chem. Geol. 97, 285–294.

Einsele, G., Yan, J., Hinderer, M., 2001. Atmospheric carbon burial in modern lake basins and its significance for the global carbon budget. Global Planet. Change. 30 (3), 167–195.

Ford, D., Williams, P., 2007. Karst Hydrogeology and Geomorphology. John Wiley, Chichester.

Gilcreas, F.W., 1966. APHA standard methods for the examination of water and waste water. Am J. Public Health. Nation's Health. 56 (3), 387–388.

Gray, D.P., Harding, J.S., Elberling, B., Horton, T., Clough, T.J., Winterbourn, M.J., 2011. Carbon cycling in floodplain ecosystems: out-gassing and photosynthesis transmit soil δ^{13}C gradient through stream food webs. Ecosystems 14 (4), 583–597.

Hotchkiss, E.R., Hall Jr., R.O., 2014. High rates of daytime respiration in three streams: use of $\delta^{18}O_{O2}$ and O_2 to model diel ecosystem metabolism. Limnol. Oceanogr. 59, 798–810.

Jiang, Y., Hu, Y., Schirmer, M., 2013. Biogeochemical controls on daily cycling of hydrochemistry and δ^{13}C of dissolved inorganic carbon in a karst spring-fed pool. J. Hydrol. 478, 157–168.

Jacobson, R., Usdowski, E., 1975. Geochemical controls on a calcite precipitating spring. Contrib. Mineral. Petrol. 51, 65–74.

Khadka, M.B., Martin, J.B., Jin, J., 2014. Transport of dissolved carbon and CO_2 degassing from a river system in a mixed silicate and carbonate catchment. J. Hydrol. 513 (11), 391–402.

Liu, H., Liu, Z., Macpherson, G.L., Yang, R., Chen, B., Sun, H., 2015. Diurnal hydrochemical variations in a karst spring and two ponds, Maolan Karst Experimental Site, China: biological pump effects. J. Hydrol. 522, 407–417.

Liu, Z., 2011. New progress and prospects in the study of rock-weathering-related carbon sinks. Chin. Sci. Bull. 57 (2–3), 95.

Martin, J.B., 2017. Carbonate minerals in the global carbon cycle. Chem. Geol. 449, 58–72.

Mook, W.G., 2006. Introduction to Isotope Hydrology. International Association of Hydrogeologists, International Contributions to Hydrogeology 25. Taylor and Francis/Balkema, London. 226 pp.

Nimick, D.A., Gammons, C.H., Parker, S.R., 2011. Diel biogeochemical processes and their effect on the aqueous chemistry of streams: a review. Chem. Geol. 283 (1), 3–17.

Odum, H.T., 1956. Primary production in flowing waters. Limnol. Oceanogr. 1 (2), 102–117.

Parker, S.R., Gammons, C.H., Poulson, S.R., DeGrandpre, M.D., 2007. Diel variations in stream chemistry and isotopic composition of dissolved inorganic carbon, upper Clark Fork River, Montana, USA. Appl. Geochem. 22 (7), 1329–1343.

Parker, S.R., Gammons, C.H., Poulson, S.R., DeGrandpre, M.D., Weyer, C.L., Smith, M.G., Babcock, J.N., Oba, Y., 2010. Diel behavior of stable isotopes of dissolved oxygen and dissolved inorganic carbon in rivers over a range of trophic conditions, and in a mesocosm experiment. Chem. Geol. 269 (1), 22–32.

Peter, H., Singer, G.A., Preiler, C., Chifflard, P., Steniczka, G., Battin, T.J., 2014. Scales and drivers of temporal pCO_2 dynamics in an Alpine stream. J. Geophys. Res. Biogeosci. 119 (6), 1078–1091.

Pu, J., Li, J., Khadka, M.B., Martin, J.B., Zhang, T., Yu, S., Yuan, D.X., 2017. In-stream metabolism and atmospheric carbon sequestration in a groundwater-fed karst stream. Sci. Total Environ. 579, 1343–1355.

Raymond, P.A., Hartmann, J., Lauerwald, R., Sobek, S., McDonald, C., Hoover, M., Butman, D., Striegl, R., Mayorga, E., Humborg, C., Kortelainen, P., Durr, H., Meybeck, M., Ciais, P., Guth, P., 2013. Global carbon dioxide emissions from inland waters. Nature 503 (7476), 355–359.

Raymond, P.A., Zappa, C.J., Butman, D., Bott, T.L., Potter, J., Mulholland, P., Laursen, A.E., McDowell, W.H., Newbold, D., 2012. Scaling the gas transfer velocity and hydraulic geometry in streams and small rivers. Limnol. Oceanogr. Fluids Environ. 2, 41–53.

Richey, J.E., Melack, J.M., Aufdenkampe, A.K., Ballester, V.M., Hess, L.L., 2002. Outgassing from Amazonian rivers and wetlands as a large tropical source of atmospheric CO_2. Nature 416 (6881), 617–620.

Schlesinger, W.H., Melack, J.M., 1981. Transport of organic carbon in the world's rivers. Tellus 33 (2), 172–187.

Smith, S.V., Gattuso, J.-P., 2011. Balancing the oceanic calcium carbonate cycle: consequences of variable water column. Aquat. Geochem. 17 (4–5), 327–337.

Sousa, W.T.Z., 2011. Hydrilla verticillata (Hydrocharitaceae), a recent invader threatening Brazil's freshwater environments: a review of the extent of the problem. Hydrobiologia 669 (1), 1–20.

Striegl, R.G., Dornblaser, M.M., McDonald, C.P., Rover, J.R., Stets, E.G., 2012. Carbon dioxide and methane emissions from the Yukon River system. Glob. Biogeochem. Cycle 26 (4) 488–488.

Tobias, C., Böhlke, J.K., 2011. Biological and geochemical controls on diel dissolved inorganic carbon cycling in a low-order agricultural stream: implications for reach scales and beyond. Chem. Geol. 283 (1), 18–30.

Tobias, C.R., Bohlke, J.K., Harvey, J.W., 2007. The oxygen-18 isotope approach for measuring aquatic metabolism in high productivity waters. Limnol. Oceanogr. 52 (4), 1439–1453.

Turner, J.V., 1982. Kinetic fractionation of carbon-13 during calcium carbonate precipitation. Geochim. Cosmochim. Acta 46 (7), 1183–1191.

van Geldern, R., Schulte, P., Mader, M., Baier, A., Barth, J.A.C., 2015. Spatial and temporal variations of pCO_2, dissolved inorganic carbon and stable isotopes along a temperate karstic watercourse. Hydrol. Process. 29 (15), 3423–3440.

Zhang, J., Quay, P.D., Wilbur, D.O., 1995. Carbon isotope fractionation during gas-water exchange and dissolution of CO_2. Geochimica. Cosmochim. Acta 59 (1), 107–114.